The Practical Application of Fractal Dimension in Water Treatment Practice-the Impact of Polymer Dosing

Peter Jarvis[a]; Simon A. Parsons[a]; Rita Henderson[a]; Nicholas Nixson[b]; Bruce Jefferson[a]

[a] Centre for Water Science Building 39, Cranfield University, Bedford, United Kingdom [b] Yorkshire Water, Bradford, United Kingdom

PLEASE SCROLL DOWN FOR ARTICLE

The Practical Application of Fractal Dimension in Water Treatment Practice – the Impact of Polymer Dosing

Peter Jarvis,[1] Simon A. Parsons,[1] Rita Henderson,[1] Nicholas Nixson,[2] and Bruce Jefferson[1]

[1]Centre for Water Science Building 39, Cranfield University, Bedford, United Kingdom
[2]Yorkshire Water, Bradford, United Kingdom

Abstract: The application of floc fractal dimension has been investigated in this work to determine if this parameter can have operational significance in water treatment. Natural organic matter suspensions were coagulated with aluminium sulphate and varying concentrations of a non-ionic polymer. The fractal dimensions of the flocs formed were measured using light scattering and settling combined with image analysis. By using the correct methodology, optimum floc properties could be determined using the floc fractal dimension combined with the floc size and strength data.

Keywords: Coagulation, floc, fractal dimension, polymer

INTRODUCTION

The use of fractal dimension (D_f) is widespread in science and many structures have been described as fractal objects. This includes a diverse range of objects including gas clouds in space (1), the mammalian lung (2), and cancerous tumours (3). Fractal structures can be defined as those that:

1.   Show self similarity regardless of the scale of investigation.

2. Show a power law relationship between two variables. This may be the relationship between the structure perimeter (P) and length (L); the area (A) and L; or the volume (V) or mass (M) and L (1–3).

$$P \propto L^{D_{FP}} \quad D_{fP} \text{ is the perimeter fractal dimension} \tag{1}$$

$$A \propto L^{D_{FA}} \quad D_{fA} \text{ is the area fractal dimension} \tag{2}$$

$$V \text{ or } M \propto L^{D_{FV}} \quad D_{fV} \text{ is the volumetric fractal dimension} \tag{3}$$

Note that D_f will take a different value dependent on the relationship investigated.
3. May be characterized by a non-integer fractal dimension.

Floc aggregates formed in water treatment have recently been studied as fractal objects and are examples of mass fractals because both the internal and surface structure exhibit fractal properties (4). The application of D_f in water treatment has focused on understanding structural changes to flocs during coagulation and flocculation and in understanding the properties of floc formed from different coagulation mechanisms. Much of the work to date has looked into idealized or synthetic systems involving model particles (such as kaolin, latex, hematite, or humic acid suspensions) because more is known about the properties of the particles investigated (5, 6). More recently work has looked at real systems looking at the floc fractal dimension of flocs formed from real river, reservoir, and lake systems (7–9).

There is still a paucity of information on how the fractal dimension can be related to operational performance in water treatment. The aim of this work was to measure the structural properties of flocs, with particular emphasis on the fractal dimension, for flocs formed from a real raw water dominated by natural organic matter (NOM) using two separate techniques (settling and light scattering). This was to enable an understanding of the structural implications of dosing polymer at increasing concentrations to the system in order to act as a floc aid. Other than changing the polymer dose, the coagulation conditions investigated matched the conditions used at the water treatment works from where the water had been collected. The values of D_f obtained were compared for each of the techniques and compared with existing data to further understand how the use of floc fractal dimension may be used from a practical viewpoint.

MATERIALS AND METHODS

Coagulation Tests

Experiments were carried out on raw water from a moorland WTWs in the north of the UK. The water was composed of a blend consisting of 70%

highly colored moorland water and 30% river water. The water had a dissolved organic carbon (DOC) content of 9.8 mg/L, ultra-violet light absorbance at 254 nm (UV_{254}) of 32.5 1/m, a zeta potential of -12.7 mV, and a turbidity of 2.0 NTU. The raw water was coagulated using aluminium sulphate at a concentration of 5.25 mg/L as Al (the dose as used by the WTWs at the time of water abstraction) from an Al stock solution of 4.25% w/w. The polymer used was a high molecular weight non-ionic polyacrylamide (Flowpam AH912). Polymer was added at concentrations between 0 and 0.25 mg/L (at the time of abstraction a dose of 0.175 mg/L was being added to the water at the WTWs in question). The coagulation pH was controlled at pH 6.0 using 0.1 M NaOH (the pH as used at the WTWs).

Coagulation and floc formation experiments were carried out on a PB-900 variable speed jar tester (Phipps and Bird) with 76×25 mm flat paddle impellers using cylindrical jars containing 1 L samples of water. An initial rapid mix was carried out at 200 rpm for 1.5 minutes. At the beginning of this period, the coagulant was added into the water. For the systems where the polymer was dosed, this was added after 1.25 minutes of the rapid mix to allow dispersion of the polymer. A slow stir period then followed at 30 rpm for 15 minutes to enable floc growth. NOM removal was assessed by measuring DOC using a Shimadzu TOC-500A analyzer and UV_{254} removal using a Jenway 6505 UV/Vis spectrophotometer. The charge of the colloids and particles in the raw water and coagulated systems were measured using a Malvern Zetasizer 2000 HAS.

Floc Size and Fractal Dimension

Floc size and growth was measured using a previously described technique (10). Briefly, a laser diffraction instrument (Malvern Mastersizer 2000) was used to measure the dynamic size of flocs with time. The suspension was measured by drawing water through the optical unit of the Mastersizer and back in to the jar using a peristaltic pump. The suspension particle size was monitored every minute following the addition of the coagulant. Measurements were logged on to a computer for further analysis. During this phase of work the impact of increased shear rate on floc properties were measured. This was carried out by increasing the rpm on the jar tester to 200 for 1 minute after the 15 minutes slow stir period. Following the high shear rate, the rpm were reduced to 30 for a further 15 minutes in order to monitor floc re-growth potential.

Floc fractal dimension was measured using two separate methods. Firstly, small angle light scattering (SALLS) was used (subsequently referred to as $D_{f(LS)}$). The determination of floc fractal dimension using SALLS has been well covered elsewhere (11, 12), so only a brief description

is provided here. The Mastersizer has a ring of photo-detectors at angles between $0.01–40.6°$ which detect light scattered by the sample. The scattered light intensity $I(Q)$ is a function of the wave number Q, where Q (m^{-1}) is the difference in magnitude of the incident and scattered laser, given by:

$$Q = \frac{4\pi n \sin(\theta/2)}{\lambda} \qquad (4)$$

Where n is the refractive index of the suspending medium, θ is the scattered angle, and λ is the wavelength of the radiation in a vacuum. For independently scattering aggregates, $I(Q)$ is related to Q and $D_{f(LS)}$:

$$I(Q) \propto Q^{-D_{f(LS)}} \qquad (5)$$

A confirmation of the power relationship in 5 is to plot I against Q on a log-log scale. A power law relationship exists if this yields a straight line, the slope of which is used to give $D_{f(LS)}$. The relationship only holds when the length of investigation is much larger than the primary particles and much smaller than the floc aggregates:

$$\frac{1}{R_{agg}} \ll Q \ll \frac{1}{R_{part}} \qquad (6)$$

R_{agg} is the radius of the aggregate and R_{part} is the radius of the primary particle.

Floc structural information was obtained from the Mastersizer during floc growth and floc breakage for all of the different polymer doses in the form of raw intensity output data which could then be converted to provide the angle of each detector and the intensity of light at each detector using a spreadsheet provided by Malvern Instruments (Malvern, UK).

The second method used to determine floc fractal dimension was established from floc sedimentation (subsequently referred to as $D_{f(S)}$). A more detailed description of the floc settling apparatus is given in (8). Briefly, flocs were grown on a jar tester as before and after 15 minutes of slow stir the flocs were carefully extracted from the jar and introduced in to a temperature controlled settling column under quiescent conditions. As flocs settled in the column, they were photographed using a CV M90 charge-coupled device camera (JAI UK). The image grabber was manually triggered to take a series of 5 images with an interval of 1 second between each frame. The projected area of the floc and the distance travelled by the floc was measured using image analysis software (Image Pro Plus from Media Cybernetics). For each polymer dose investigated, the settling rate of between $56–100$ flocs were measured.

Floc $D_{f(S)}$ was measured from the settling rate based on the relationship between the diameter of a floc (d) and its terminal settling velocity (V_t) (7).

A log-log plot of settling velocity against floc diameter yields a straight line with a slope of $D_{f(S)} - 1$.

$$V_t \propto d^{D_{f(S)}-1} \tag{7}$$

For both methods of measuring floc fractal dimension, a mass fractal is given where D_f can take values between 1 and 3. A higher value of D_f indicates a more compact structure, whilst lower values indicate a more open and stringy structure.

RESULTS

Coagulation Tests

The removal of NOM with increasing polymer dose for this raw water was seen to increase with increasing polymer dose (Table 1). The percentage removal of DOC (46–58%) was much lower than for the removal of UV_{254} absorbing compounds (84–88%). This reflects that UV_{254} absorbing NOM can be more easily removed by coagulation due to the increased charge and higher MW (molecular weight) of this type of NOM when compared to the non-UV_{254} absorbing NOM which is normally composed of smaller MW and un-charged compounds. These compounds are usually recalcitrant to removal by coagulation. The reduction of the magnitude of the negative charge of the zeta potential from -12.7 mV to $+1.3$ mV with increasing polymer dose was interesting given that the polymer used was non-ionic. However, given that the floc properties were significantly different with an increase in polymer dose, the increase in the zeta potential was likely to be a reflection of the improved NOM removal seen at higher polymer doses through better adsorption/exchange of NOM on to the larger flocs formed at higher polymer dose (Fig. 1).

Table 1. Removal performance of the different treatment systems with increasing polymer

| Floc system–polymer dose added mg/L	DOC mg/L (% removal in brackets)	UV_{254} 1/m (% removal in brackets)	Zeta potential mV
Raw water	9.8	32.5	-12.7
0	5.4 (46%)	5.6 (84%)	-9.6
0.05	5.6 (43%)	5.1 (84%)	-7.1
0.10	5.5 (44%)	4.3 (87%)	-4.7
0.15	5.3 (46%)	3.5 (89%)	0.5
0.20	4.1 (58%)	4.0 (88%)	-0.5
0.25	3.6 (64%)	4.1 (87%)	1.3
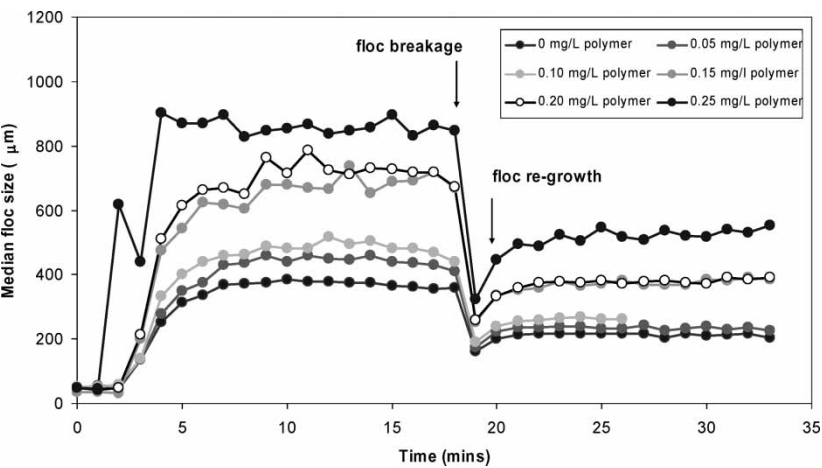
Figure 1. Floc growth, breakage and regrowth with time for increasing polymer doses.

Floc Size and Fractal Dimension

The floc size was seen to increase with increasing polymer dose (Fig. 1). When no polymer was dosed, the median floc size at the end of the slow stir period was 358 μm, this increased to 849 μm for the highest polymer dose of 0.25 mg/L. The biggest change in floc size was observed when the polymer dose was increased from 0.10 mg/L to 0.15 mg/L which resulted in an increase in median floc size of 230 μm. When the floc suspensions were exposed to an increase in shear rate of 200 rpm, the flocs broke, but the response was dependent on polymer dose. The systems dosed with 0.10 mg/L polymer and below broke to a similar size (160–190 μm). At polymer doses of 0.15–0.20 mg/L the flocs broke to 260 μm whilst the highest polymer dose only broke to a size of 320 μm. There was little difference in the floc regrowth potential of each of the systems. Although the higher polymer doses regrew to larger floc sizes, all of the flocs reached between 55–65% of the previous size reached after the initial 15 minutes slow stir. The incapacity of the floc system to regrow to the size seen previously is an observation seen before and is thought to result as flocs re-structure during breakage, resulting in fewer active bonding sites being available for reattachment (13, 14).

Examples of the derivation of floc fractal dimension from the log-log plot of scattered light intensity ($Q(I)$) against wave number (Q) are shown in Fig. 2 for the systems containing no polymer and the highest polymer dose (0.25 mg/L). For all calculations of $D_{f(LS)}$), the correlation co-efficient of the regression line was high ($R^2 > 0.99$) indicating highly significant relationships between the two parameters. The fractal dimensions obtained using SALLS for each of the polymer doses are shown in Table 2.
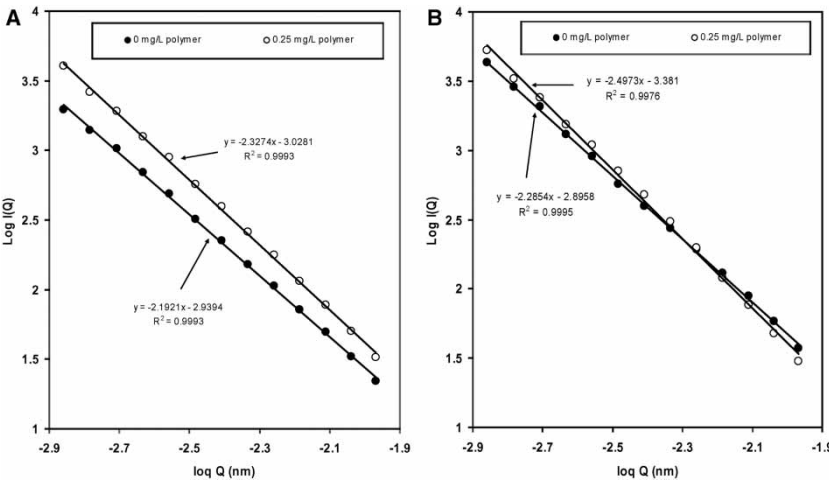
Figure 2. The relationship between the scattered light intensity (I) and the wave number (Q) on a log-log scale and the determination of the fractal dimension for different flocs during the initial growth phase (A) and breakage phase (B) for i) flocs formed with no polymer added and ii) the highest polymer dose added.

Table 2. Fractal dimension values as calculated using SALLS during floc growth, breakage and re-growth and the fractal value obtained from floc settling

|	Fractal Dimension				
	Salls				Settlement
Floc system-Polymer dose added	Growth (95% CI on slope)	Max floc size (95% CI on slope)	Breakage (95% CI on slope)	Re-growth (95% CI on slope)	Max floc size (95% CI on slope)
0 mg/L	2.19 (2.15–2.23)	2.45 (2.37–2.52)	2.28 (2.25–2.32)	2.46 (2.35–2.57)	1.70 (1.56–1.86)
0.05 mg/L	2.18 (2.14–2.22)	2.40 (2.35–2.45)	2.27 (2.23–2.31)	2.42 (2.31–2.53)	1.56 (1.45–1.67)
0.10 mg/L	2.20 (2.16–2.24)	2.41 (2.39–2.44)	2.31 (2.26–2.36)	2.39 (2.39–2.47)	1.87 (1.72–2.04)
0.15 mg/L	2.32 (2.35–2.30)	2.40 (2.36–2.44)	2.37 (2.30–2.44)	2.38 (2.31–2.47)	1.74 (1.64–1.87)
0.20 mg/L	2.26 (2.23–2.29)	2.37 (2.33–2.41)	2.36 (2.29–2.44)	2.36 (2.30–2.42)	1.95 (1.86–2.04)
0.25 mg/L	2.33 (2.29–2.37)	2.34 (2.32–2.37)	2.50 (2.42–2.58)	2.38 (2.31–2.45)	—

The $D_{f(LS)}$ value was seen to increase with increasing polymer dose during the growth phase (measurement taken from minute 4 in Fig. 1) from 2.19 to 2.33 with increasing polymer dose. The biggest increase in $D_{f(LS)}$ was from an increase in polymer dose from 0.10 to 0.15 mg/L. It was interesting to note that for all systems the fractal value increased as the flocs grew to their maximum size (measurement taken after 15 minutes of growth). However, the order of $D_{f(LS)}$ reversed after 15 minutes of floc growth (i.e. the maximum floc size for each system) with the no polymer and lowest polymer doses having the biggest increase and highest value of $D_{f(LS)}$. When the flocs where broken the $D_{f(LS)}$ value decreased for most of the polymer systems, however, this was dependent on the polymer dose. For example, when no polymer was added, $D_{f(LS)}$ decreased from 2.45 to 2.28; however, the extent of this change was reduced with increasing polymer dose such that the $D_{f(LS)}$ value did not significantly change at doses of 0.15 and 0.20 mg/L. The highest polymer dose showed an increase in $D_{f(LS)}$ during the breakage phase from 2.34 to 2.50. After the floc re-growth period, the floc fractal dimension returned to values previously seen for the maximum floc size.

The floc settling distribution with increasing floc size for each polymer dose is shown in Fig. 3. The fractal values obtained for flocs from settling were those for fully grown flocs formed after 15 minutes on a jar tester (Table 2). The trend in $D_{f(S)}$ generally showed an increase in floc fractal dimension with increasing polymer dose; the reverse of that was seen using SALLS. When no polymer was dosed, the $D_{f(S)}$ was 1.70; however, there was a high degree of uncertainty on this value (analysis of the 95% confidence interval (CI) on the slope of this line indicated that the fractal dimension could have taken a value between 1.56–1.86). At a polymer dose of 0.05 mg/L the $D_{f(S)}$ was 1.55 (95% CI, 1.45–1.67). At higher polymer doses between 0.10 and 0.15 mg/L, the $D_{f(S)}$ increased to 1.87 (95% CI, 1.72–2.04) and 1.74 (95% CI, 1.64–1.87) respectively, indicating a trend of more compaction with increasing polymer dose. At 0.20 mg/L the $D_{f(S)}$ value was significantly higher at 1.96 (95% CI, 1.86–2.04). Interrogation of the 95% CI of the slope indicated that the highest polymer dose had a significantly larger $D_{f(S)}$ than the no polymer system and the lowest dose of 0.05 mg/L.

DISCUSSION

Polymer dosing into pre-clarified water is a widely used tool in drinking water treatment to aid floc formation and improve the removal of these aggregates during the clarification processes. Therefore, as may be expected, the WTWs investigated in this work sees better clarification performance when polymer is dosed compared to when it is not dosed (15). The particle sizing results clearly showed an increase in floc size and improved resistance to increased shear rate with increasing polymer dose. Improved resistance to
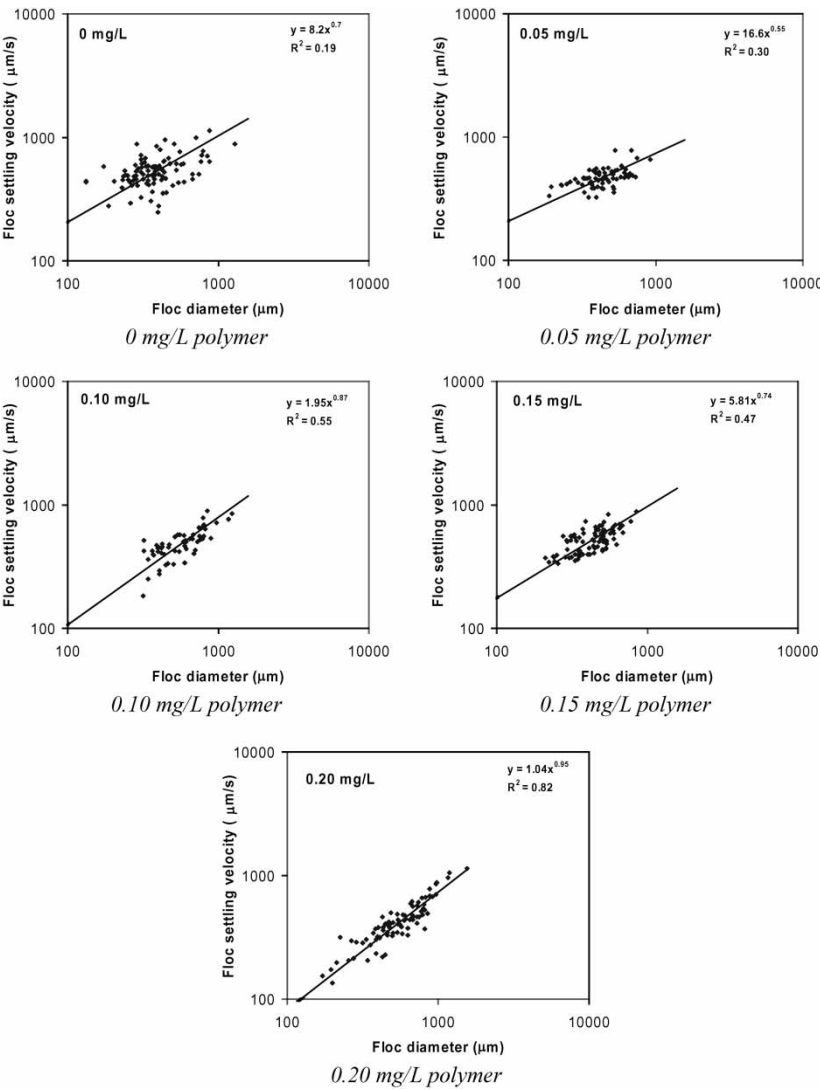
Figure 3. The relationship between settling rate and floc size for systems with increasing polymer dose.

increased shear rate was apparent because polymer dosed systems were able to maintain a larger average size after exposure to a high shear rate (200 rpm). The impact of larger floc size and improved resistance to shear rate with increasing polymer dose can be seen to have a clear link with plant operational performance. For example, a greater number of larger flocs will clarify better, particularly in sedimentation clarification systems (16). However, the operational significance of D_f was less clear.

A highly heterogeneous system has been analyzed in this work (with NOM of different MW, coagulant-NOM precipitates and turbidity components contributing to the overall floc structure), it is likely that the primary particles that make up the floc are of a similar structure (relatively homo-dispersed primary particles composed of a heterogeneous mixture of components).

The $D_{f(S)}$ values reported were significantly lower than those obtained using SALLS which is a result consistent with other studies (12). The difference is due to the fact that fractal dimension is an operationally defined value based on the method used to generate the value. The $D_{f(LS)}$ generated from SALLS refers to the structure of the floc aggregates over a small length scale whilst that determined by settling refers to the global structure of the overall floc.

The two different techniques for measuring floc fractal dimension gave contrasting trends in that the $D_{f(LS)}$ decreased with an increasing polymer dose whilst there were indications that $D_{f(S)}$ increased with increasing polymer concentration. As seen in previous studies, the spread of the data for determination of fractal dimension was much greater for settlement when compared to SALLS as reflected by low correlation co-efficients for the regression line through the data (Fig. 3) (17). This is as a result of a number of factors influencing floc settlement behaviour such as floc orientation and advection effects. For the lowest polymer dose, which resulted in the smallest floc, there was the most scatter ($R^2 = 0.18$). This was because when no polymer was dosed there was a more inconsistent floc structure and a weaker overall aggregate. The floc were therefore more susceptible to changes in environmental conditions during the measurement procedure (17). For this type of scattered system, the fractal dimension number is probably an average of a range of values taken by the floc in the system. When polymer was added the relationship became stronger with R^2 co-efficients of >0.30 and this increased to a highly significant relationship at 0.20 mg/L polymer ($R^2 = 0.82$) as a result of a more consistent floc structure as polymer was dosed.

The difference in the D_f measured from the two different techniques was a reflection that the fractal dimension of different sized aggregates was being measured in the (4). The resolution of the image analysis system used with the floc settling apparatus was only able to measure the properties of floc $>100 \, \mu m$. For SALLS the $D_{f(LS)}$ of the microflocs in the system were measured (from Equation (6), typically of flocs that were $<10 \, \mu m$ (8, 12). The results therefore show that the small microflocs within the whole floc became more open as the polymer dose was increased, whilst the overall floc becomes more compact as polymer dose was increased. As was indicated here, previous work has shown that an increase in polymer dose usually results in an increase in overall floc fractal dimension (18, 19). However, most work has shown an increase in microfloc fractal dimension with increasing polymer dose when

SALLS has been used (12, 18, 20). This difference was likely to be explained because these previous workers used the polymers as the principal coagulant or because of charge differences in the properties of the polymers used. Polymer bridging was the most likely mechanism for bonding by the non-ionic polymer used in this work due to the increased probability of attachment in these polymers (21). In this case, increased polymer dosing appeared to give a more open structure for the microflocs formed after 15 minutes growth as a result of polymer bridging giving more tenuous bonding (12). The fractal dimension of microflocs during breakage stayed the same at low polymer dose or increased for systems of high polymer dose where the overall floc size was very large (polymer doses of ≥ 0.15 mg/L). It was hypothesized that increased polymer bridging within the microfloc at high polymer dose held the aggregates together under the high breakage shear rate due to the strong bonding of the polymer. For the microfloc in the systems with low or no polymer dose an opening up of these structures was seen at higher shear rates due to the weaker bonding in the floc when little or no polymer was present.

The increase in the overall $D_{f(S)}$ of the whole floc as found from settling with increasing polymer dose indicated that the polymer bridging within the overall floc produced more compact aggregates. The exception here was for the no polymer dosed system, that appeared to have a high fractal dimension but the high scatter and low correlation co-efficient make this value very questionable. This indicated that in the small floc systems with low concentrations, the more compact microflocs have weaker inter-bonding forces between the microfloc giving rise to a smaller, inconsistent, and more loosely connected overall aggregate. At higher concentrations of polymer, the increased magnitude and strength of bridging bonds was likely to give a stronger and overall more compact structure.

From a practical perspective, polymer is frequently used in order to increase floc size and result in a distribution of fewer smaller particles in order to increase floc strength and settlement (21). The fractal dimension analysis used in this work suggested that SALLS analysis should be restricted to the small microflocs in the system. Settling gives a better understanding of the properties of the whole floc in the system and is therefore of more operational use because it is the removal of the bulk of the flocs that is important during clarification. Importantly, care must be taken with settling data to understand if there is a significant relationship between the settling rate and floc size and an understanding of the range of values that the fractal dimension may take to determine if there are significant differences between D_f from different systems. In this work, the fractal dimension analysis identified an increase in the compaction of the whole floc with increasing polymer dose; however, there was only a statistically significant increase between the low and high polymer doses. The fractal value must also be used in combination with floc size, strength, and settling rate data in

order to give a complete understanding of how floc operational properties change with different variables.

ACKNOWLEDGMENTS

REFERENCES

1. De Vega, H.J., Sánchez, N., and Combes, F. (1996) Self-gravity as an explanation of the fractal structure of the interstellar medium. *Nature*, 383 (6595): 56–58.
2. Muroy, B., Filoche, M., Welbel, E.R., and Sapoval, B. (2004) An optimal bronchial tree may be dangerous. *Nature*, 427 (6975): 633–636.
3. Kikuchi, A., Kozuma, S., Yasugi, T., and Taketani, Y. (2006) 3-D fractal tumour growth of epithelial ovarian cancer. *European Journal of Gynaecological Oncology*, 27 (6): 561–565.
4. Jefferson, B. and Jarvis, P. (2006) Practical application of fractal dimension. In *Interface Science in Drinking Water Treatment: Theory and Applications*; Newcombe, G. and Dixon, D. (eds.); Academic Press, Elsevier Ltd: Oxford, UK.
5. Tang, S. (1999) Prediction of fractal properties of polystyrene aggregates. *Colloids and Surface A: Physiochemical and Engineering Aspects*, 157: 27–41.
6. Lee, S.A., Fane, A.G., and Waite, T.D. (2005) Impact of natural organic matter on floc size and structure effects in membrane filtration. *Environmental Science and Technology*, 39 (17): 6477–6486.
7. Ho, L. and Newcombe, G. (2005) Effect of NOM, turbidity and floc size on the PAC adsorption of MIB during alum coagulation. *Water Research*, 39 (15): 3668–3674.
8. Jarvis, P., Jefferson, B., and Parsons, S.A. (2005a) The impact of the natural organic matter to coagulant ratio on floc structural properties. *Environmental Science and Technology*, 39: 8919–8924.
9. Chakraborti, R.K., Gardner, K.H., Kaur, J., and Atkinson, J.F. (2007) In situ analysis of flocs. *Journal of Water Supply: Research and Technology–AQUA*, 56 (1): 1–11.
10. Jarvis, P., Jefferson, B., and Parsons, S.A. (2005b) Breakage, re-growth and fractal nature of natural organic matter flocs. *Environmental Science and Technology*, 39: 2307–2314.
11. Waite, T.D., Cleaver, J.K., and Beattie, J.K. (2001) Aggregation kinetics and fractal structure of γ-alumina assemblages. *Colloid and Interface Science*, 241: 333–339.
12. Wu, R.M., Lee, D.J., Waite, T.D., and Guan, J. (2002) Multilevel structure of sludge flocs. *Journal of Colloid and Interface Science*, 252: 383–392.
13. Yeung, A.K.C., Gibbs, A., and Pelton, R.P. (1997) Effect of shear on the strength of polymer-induced flocs. *Journal of Colloid and Interface Science*, 196: 113–115.
14. Spicer, P.T., Pratsinis, S.E., Raper, J., Amal, R., Bushell, G., and Meesters, G. (1998) Effect of shear schedule on particle size, density and structure during flocculation in stirred tanks. *Powder Technology*, 97: 26–34.
15. Nixson, N. (2007). Personal communication.

16. Aguilar, M.I., Saez, J., Llorens, M., Soler, A., and Ortuno, J.F. (2003) Microscopic observation of particle reduction in slaughterhouse wastewater by coagulation-flocculation using ferric sulfate as coagulant and different coagulant aids. *Water Research*, 37: 2233–2241.

17. Liao, J., Selomulya, C., Bushell, G., Bickert, G., and Amal, R. (2005) On different approaches to estimate the mass fractal dimension of coal aggregates. *Particle and Particle Systems Characterization*, 22 (5): 299–309.

18. Glover, S.M., Yan, Y-D., Jameson, G.J., and Biggs, S. (2000) Bridging flocculation studied by light scattering and settling. *Chemical Engineering Journal*, 80 (1–3): 3–12.

19. Zhao, Y.Q. (2004) Settling behavior of polymer flocculated water-treatment sludge II: Effects of floc structure and floc packing. *Separation and Purification Technology*, 35 (3): 175–183.

20. Waite, T.D. (1999) Measurement and implications of floc structure in water and wastewater treatment. *Colloids and Surfaces A: Physicochemical and Engineering Aspects*, 151 (1–2): 27–41.

21. Besra, L., Sengupta, D.K., Royb, S.K., and Ayc, P. (2004) Influence of polymer adsorption and conformation on flocculation and dewatering of kaolin suspension. *Separation and Purification Technology*, 37 (3): 231–246.